Magnetic-Field Induced Efficient Alignment of Carbon Nanotubes in Aqueous Solutions

Krisztián Kordás,*,† Tero Mustonen,† Géza Tóth,† Jouko Vähäkangas,† Antti Uusimäki,† Heli Jantunen,† Amita Gupta,‡ K. V. Rao,‡ Róbert Vajtai,§ and Pulickel M. Ajayan⊥

Microelectronics and Materials Physics Laboratories and EMPART research group of Infotech Oulu, Department of Electrical and Information Engineering, University of Oulu, FIN-90014 University of Oulu, Finland, Department of Materials Science-Tmfy-MSE, Royal Institute of Technology, SE-10044 Stockholm, Sweden, and Rensselaer Nanotechnology Center and Department of Materials Science & Engineering, Rensselaer Polytechnic Institute, Troy, New York 12180

Received September 14, 2006. Revised Manuscript Received November 21, 2006

Efficient alignment of aqueous carboxyl-functionalized multiwalled carbon nanotubes having remanent iron catalyst particles are carried out in relatively low external magnetic fields ($B \leq 1017$ mT). The nanotubes were grown by catalytic chemical vapor deposition and then functionalized in a multistep oxidation process using nitric acid and potassium permanganate. In the field-induced ordering, the ferromagnetic property of iron nanoparticles entrapped in the inner-tubular cavity of nanotubes is exploited. Considerable dichroism of nanotube solutions (up to 3.02) is measured and deposition of aligned CNT networks from the solutions on silicon substrates is demonstrated.

Introduction

Synthesis of aligned carbon nanotube (CNT) architectures is of great importance in order to exploit their anisotropic electrical, mechanical, optical, and thermal properties in future devices.[1−10] To achieve ordering, one approach is a direct growth of aligned CNT films by catalytic chemical vapor deposition (CCVD) from organic precursors over metal catalyst particles (Fe, Co, Ni, Pd, and their blends) on a Si/SiO_2 support[11−14] or by the decomposition of organometallic compounds.[15,16] Further ordering of CNTs into macroscopic ropes and belts is also possible by simply pulling yarns from the aligned nanotube films.[17] The macroscopic films/ropes found direct applications in field-emission devices[18] and optical polarizers[19] and enable an easy synthesis of anisotropic composites by embedding the nanotube structures in polymers or ceramics.[20−22]

Nanotubes either dissolved or dispersed in a solvent, which is often the case when CNTs are subjected to chemical modifications, have random orientation in the liquid medium. Several alternatives have been reported for ordering random systems, such as spinning of suspended CNTs pretreated with fuming sulfuric acid,[23] condensing of viscous flow-aligned polymer−nanotube composites,[24] and using the cooperative

* Corresponding author. E-mail: lapy@ee.oulu.fi. Fax: 358 8 5532728. Tel: 358 8 5532723.
† University of Oulu.
‡ Royal Institute of Technology.
§ Rensselaer Nanotechnology Center, Rensselaer Polytechnic Institute.
⊥ Department of Materials Science & Engineering, Rensselaer Polytechnic Institute.

(1) Xie, X.-L.; Mai, Y.-W.; Zhou, X.-P. *Mater. Sci. Eng., R* **2005**, *49*, 89.
(2) Wang, X.; Liu, Y.; Yu, G.; Xu, C.; Zhang, J.; Zhu, D. *J. Phys. Chem. B* **2001**, *105*, 9422.
(3) Zhao, G. L.; Bagayoko, D.; Yang, L. *J. Appl. Phys.* **2006**, *99*, 114311.
(4) Murakami, Y.; Einarsson, E.; Edamura, T.; Maruyama, S. *Phys. Rev. Lett.* **2005**, *94*, 87402.
(5) Islam, M. F.; Alsayed, A. M.; Dogic, Z.; Zhang, J.; Lubensky, T. C.; Yodh, A. G. *Phys. Rev. Lett.* **2004**, *92*, 88303.
(6) Hone, J.; Llaguno, M. C.; Nemes, N. M.; Johnson, A. T.; Fischer, J. E.; Walters, D. A.; Casavant, M. J.; Schmidt, J.; Smalley, R. E. *Appl. Phys. Lett.* **2000**, *77*, 666.
(7) Gonnet, P.; Liang, Z.; Choi, E. S.; Kadambala, R. S.; Zhang, C.; Brooks, J. S.; Wang, B.; Kramer, L. *Curr. Appl. Phys.* **2006**, *6*, 119.
(8) Bubke, K.; Gnewuch, H.; Hampstead, M.; Hammer, J.; Green, M. L. H. *Appl. Phys. Lett.* **1997**, *71*, 1906.
(9) Fischer, J. E.; Zhou, W.; Vavro, J.; Llaguno, M. C.; Guthy, C.; Haggenmueller, R.; Casavant, M. J.; Walters, D. A.; Smalley, R. E. *J. Appl. Phys.* **2003**, *93*, 2157.
(10) Shi, D.; He, P.; Lian, J.; Chaud, X.; Bud'ko, S. L.; Beaugnon, E.; Wang, L. M.; Ewing, R. C.; Tournier, R. *J. Appl. Phys.* **2005**, *97*, 64312.
(11) Srivastava, A.; Srivastava, O. N.; Talapatra, S.; Vajtai, R.; Ajayan, P. M. *Nat. Mater.* **2004**, *3*, 610.
(12) Wei, B. Q.; Vajtai, R.; Jung, Y.; Ward, J.; Zhang, R.; Ramanath, G.; Ajayan, P. M. *Chem. Mater.* **2003**, *15*, 1598.
(13) Kordás, K.; Tóth, G.; Moilanen, P.; Kumpumäki, M.; Vähäkangas, J.; Uusimäki, A.; Vajtai, R.; Ajayan, P. M. **2007**, submitted for publication.
(14) Wei, B. Q.; Vajtai, R.; Jung, Y.; Zhang, W.; Ramanath, G.; Ajayan, P. M. *Nature* **2002**, *416*, 495.
(15) Rao, C. N. R.; Govindaraj, A. *Acc. Chem. Res.* **2002**, *35*, 998.
(16) Rao, C. N. R.; Sen, R.; Satishkumar, B. C.; Govindaraj A. *Chem. Commun.* **1998**, 1525.
(17) Zhang, M.; Fang, S.; Zakhidov, A. A.; Lee, S. B.; Aliev, A. E.; Williams, C. D.; Atkinson, K. R.; Baughman, R. H. *Science* **2005**, *309*, 1215.
(18) Deheer, W. A.; Chatelain, A.; Ugarte, D. *Science* **1995**, *270*, 1179.
(19) Ichida, M.; Mizuno, S.; Kataura. H.; Achiba, Y.; Nakamura, A. *Appl. Phys. A* **2004**, *78*, 1117.
(20) Jung, Y. J.; Kar, S.; Talapatra, S.; Soldano, C.; Viswanathan, G.; Li, X.; Yao, Z.; Ou, F. S.; Avadhanula, A.; Vajtai, R.; Curran, S.; Nalamasu, O.; Ajayan, P. M. *Nano Lett.* **2006**, *6*, 413.
(21) Veedu, V. P.; Cao, A.; Li, X.; Ma, K.; Soldano, C. Kar, S.; Ajayan, P. M.; Ghasemi-Nejhad, M. N. *Nat. Mater.* **2006**, *5*, 457.
(22) Hinds, B. J.; Chopra, N.; Rantell, T.; Andrews, R.; Gavalas, V.; Bachas, L. G. *Science* **2004**, *303*, 62.
(23) Ericson, L. M.; Fan, H.; Peng, H.; Davis, V. A.; Zhou, W.; Sulpizio, J.; Wang, Y.; Booker, R.; Vavro, J.; Guthy, C.; Nicholas, A.; Parra-Vasquez, G.; Kim, M. J.; Ramesh, S.; Saini, R. K.; Kittrell, C.; Lavin, G.; Schmidt, H.; Adams, W. W.; Billups, W. E.; Pasquali, M.; Hwang, W.-F.; Hauge, R. H.; Fischer, J. E.; Smalley, R. E. *Science* **2004**, *305*, 1447.

10.1021/cm062196t CCC: $37.00
Published on Web 01/17/2007

reorientation of liquid crystal−CNT suspensions in an electric field.[25] Direct alignment with external electrostatic or magnetic fields also offers a plausible way to induce ordering, as was demonstrated for single-walled CNT suspensions.[6−10,26−29] It is, however, worth pointing out that in the case of CNTs without ferromagnetic catalyst impurities, very large magnetic flux densities ($B > 10$ T) are necessary to achieve considerable ordering.[7,9,29−31] This is due to the low magnetic polarization originating from the paramagnetic behavior, what undermines, or at least greatly limits, the possibilities of magnetic alignment in practical applications. To overcome the difficulties arising from the low intrinsic magnetization of CNTs, other research groups have shown that ferromagnetic particles can be linked to the nanotubes' surfaces or, alternatively, the inter-tubular cavity can be filled with magnetic fluids in subsequent multistep processes.[32−34]

In this paper, we demonstrate an efficient alignment of aqueous carboxyl functionalized multiwalled CNTs induced by relatively low magnetic fields ($B \leq 1017$ mT). The alignment accomplished by our method has three remarkable features:

- The low magnetic flux density we apply to align the nanotubes makes the process practical, contrary to the several Tesla (in some cases tens of Tesla) fields applied for pure nanotubes.
- We exploit the ferromagnetic behavior of residual iron nanoparticles entrapped in the inner-tubular cavity of nanotubes, thus avoiding multistep postdeposition processes toward anchored magnetic nanoparticles on the nanotubes made in other works. Inherently, our process minimizes the amount of extrinsic materials; the advantageous properties of CNTs are therefore preserved.
- The medium in which the nanotubes are dissolved is water, enabling versatile applications in various fields. The applied aqueous solutions of carboxyl-functionalized nanotubes avoid contaminations and side effects arising from the nonvolatile solvents or additives.

Experimental Section

In our experiments, multiwalled carbon nanotubes (MWCNTs) with lengths of 1−2 mm and outer diameters of 10−70 nm were used. The nanotubes were grown by CCVD on Si/SiO_2 wafers in a tube reactor at 770 °C from a precursor of xylene and ferrocene mixture (10 g L^{-1}).[12−14] The synthesized films of aligned MWCNTs were detached from the templates by dissolving the SiO_2 surface in a mixture of hydrofluoric acid and ethanol (3:7 vol/vol). The freestanding nanotube mats were thoroughly flushed in ethanol and dried with pressurized nitrogen. The obtained pristine CNTs were processed further in a multistep oxidation procedure to decrease the amount of catalyst iron particles co-deposited during the nanotube synthesis and introduce carboxyl functional groups, i.e., to obtain carboxylated CNTs. A typical procedure for carboxylation follows the same routine we used for generating printable nanotube inks.[35] MWCNTs were sonicated for 10 min and then refluxed in cc. HNO_3 for 24 h (20 mg of CNT in 20 mL of HNO_3). The product was diluted with 200 mL of deionized (DI) water, filtered with coarse filter paper, washed with DI water until it reached pH ∼7, and finally dried at 120 °C for 4 h. To complete the oxidation of hydroxyl and carbonyl groups, which form besides carboxyl groups, the samples were sonicated in 10 mL of DI water, and a $KMnO_4$ solution (45 mg of $KMnO_4$ in 10.5 mL of 70% $HClO_4$) was added. After 10 min of stirring, a citric acid solution (21 mL, 0.0148 M) was added to quench $KMnO_4$. Finally, the product, i.e., carboxylated nanotubes CNT-$(COOH)_n$, was filtered and washed with DI water. To make aqueous solutions, we first sonicated the functionalized nanotubes (10 mg) in 10 mL of DI water for half an hour, followed by stirring for 24 h and centrifuging at 4000 rpm for 15 min. The supernatant solution was collected and centrifuged again. The procedure was repeated until a stable homogeneous solution was achieved (typically 4 times). The obtained dark gray but transparent stock solution having a MWNT-$(COOH)_n$ concentration of ∼0.26 mg mL^{-1} proved to be stable for over several days of storage. According to field-emission scanning electron microscopy (FESEM) analysis of dried solution droplets, the length of dissolved nanotubes is between 1 and 5 μm.

Results and Discussion

As revealed by SQUID analyses (MPMS2, superconducting quantum interference device; Quantum Design), our nanotubes show ferromagnetic polarization with a saturation M_s of 0.65 emu g^{-1} at 300 K and 0.77 emu g^{-1} at 5 K, which decreases to 0.12 emu g^{-1} at 300 K and to 0.17 emu g^{-1} at 4 K after the carboxylation process (Figure 1). Because the nanotubes themselves are paramagnetic, the ferromagnetic behavior is attributed to the iron catalyst particles co-deposited with the nanotubes during the growth. The reduced magnetization found for the carboxyl-functionalized CNTs is due to the partial dissolution of Fe nanoparticles in nitric acid. However, despite the elongated acidic oxidation, some residual Fe remains entrapped in the nanotubes yielding a nonvanishing ferromagnetic polarization for such samples. The reduced Fe content in the treated CNTs is confirmed by SEM/EDS analyses (Jeol JSM-6400, EDS Inca), which showed an average Fe concentration of 0.23 ± 0.03 and 0.08 ± 0.03 at % before and after oxidation, respectively. The entrapped catalyst particles are usually rod-shaped with a typical diameter of 5−10 nm (the same as the inner cavity diameter) and length of 10−50 nm (see the Supporting Information, Figure S1).

(24) Vigolo, B.; Pénicaud, A.; Coulon, C.; Sauder, C.; Pailler, R.; Journet, C.; Bernier, P.; Poulin, P. *Science* **2000**, *290*, 1331.
(25) Dierking, I.; Scalia, G.; Morales, P. *J. Appl. Phys.* **2005**, *97*, 44309.
(26) Islam, M. F.; Milkie, D. E.; Kane, C. L.; Yodh, A. G.; Kikkawa, J. M. *Phys. Rev. Lett.* **2004**, *93*, 37404. Islam, M. F.; Milkie, D. E.; Kane, C. L.; Yodh, A. G.; Kikkawa, J. M. *Phys. Rev. Lett.* **2005**, *94*, 19901(E).
(27) Kamat, P. V.; Thomas, K. G.; Barazzouk, S.; Girishkumar, G.; Vinodgopal, K.; Meisel, D. *J. Am. Chem. Soc.* **2004**, *126*, 10757.
(28) Takahasi, T.; Murayama, T.; Higuchi, A.; Awano, H.; Yonetake, K. *Carbon* **2006**, *44*, 1180.
(29) Walters, D. A.; Casavant, M. J.; Quin, X. C.; Huffman, C. B.; Boul, P. J.; Ericson, L. M.; Haroz, E. H.; O'Connel, M. J.; Smith, K.; Colbert, D. T.; Smalley, R. E. *Chem. Phys. Lett.* **2001**, *338*, 14.
(30) Fujiwara, M.; Oki, E.; Hamada, M.; Tanimoto, Y.; Mukouda, I.; Shimomura, Y. *J. Phys. Chem. A.* **2001**, *105*, 4383.
(31) Zaric, S.; Ostojic, G. N.; Kono, J.; Shaver, J.; Moore, V. C.; Hauge, R. H.; Smalley, R. E.; Wei, X. *Nano Lett.* **2004**, *4*, 2219.
(32) Correa-Duarte, M. A.; Grzelczak, M.; Salgueirino-Maceira, V.; Giersig, M.; Liz-Marzan, L. M.; Farle, M.; Sierazdki, K.; Diaz, R. *J. Phys. Chem. B* **2005**, *109*, 19060.
(33) Gao, C.; Li, W.; Morimoto, H.; Nagaoka, Y.; Maekawa, T. *J. Phys. Chem. B* **2006**, *110*, 7213.
(34) Korneva, G.; Ye, H.; Gogotsi, Y.; Halverson, D.; Friedman, G.; Bradley, J.-C.; Kornev, K. G. *Nano Lett.* **2005**, *5*, 879.
(35) Kordás, K.; Mustonen, T.; Tóth, G.; Jantunen, H.; Lajunen, M.; Soldano, C.; Talapatra, S.; Kar, S.; Vajtai, R,; Ajayan, P. M. *Small* **2006**, *2*, 1021.

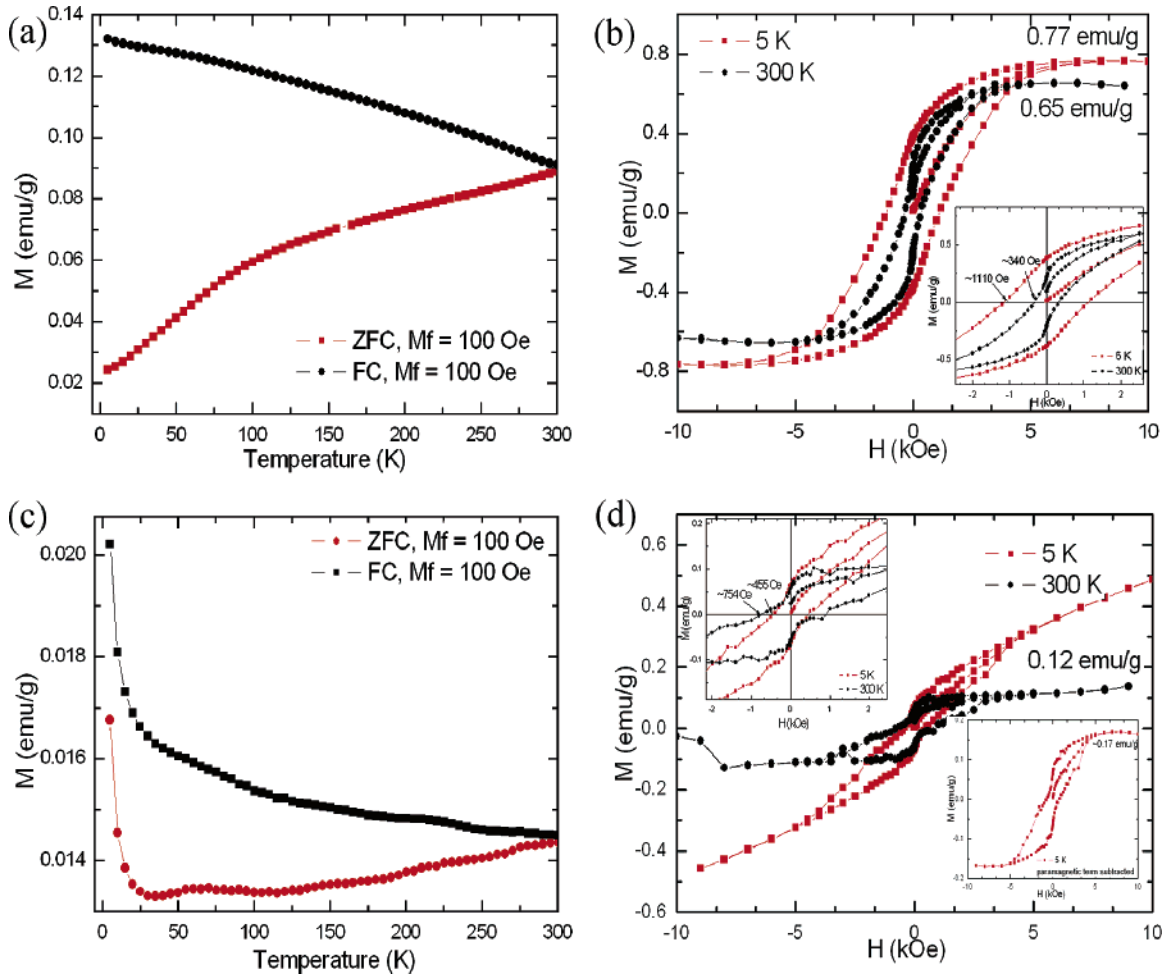

Figure 1. Temperature dependence of magnetization $M(T)$ for (a) pristine and (c) carboxyl-functionalized, i.e., acid-treated, nanotubes, measured for both zero-field cooling, ZFC, and field cooling, FC. Field dependence of magnetization $M(H)$ for (b) pristine and (d) acid-treated nanotubes measured at 5 and 300 K. The lower inset in panel (b) and upper inset in panel (d) show a magnified $M(H)$ plot for low fields near the origin revealing the finite coercivity, H_c value. The lower inset of panel (d) shows the ferromagnetic term at 5 K as extracted from (d).

The magnetization curves for both pristine and carboxylated nanotubes show hysteresis, confirming ferromagnetic ordering for all temperatures from 5 to 300 K (panels b and d of Figure 1). For both cases, these hysteresis loops are constricted, indicating the presence of more than one ferromagnetic phase with different coercivities. A possibility is the presence of ferromagnetic oxides of iron, Fe_2O_3 or Fe_3O_4, along with Fe particles. For the carboxylated nanotubes, an additional paramagnetic phase is present at 5 K that shows up in the $M(H)$ curve at high fields (Figure 1d) as a linear term. This is also evident from the temperature dependence of magnetization shown in Figure 1c, where an increase in magnetization is seen in both zero-field-cooled (ZFC) and field-cooled (FC) curves at low temperatures. This is in good agreement with previous studies,[31] in which enhanced paramagnetic behavior was found for nanotubes exposed to electron irradiation and acid treatment because of the formation of defects in the graphene lattice and dangling bonds on the tubes' surface, both of which result in a change in the density of states at the Fermi level. Such defects act as localized magnetic moments with Curie-type behavior.[36−39]

The considerable magnetic polarization in our acid-treated CNTs gives rise to induced spatial alignment, i.e., nematic ordering of nanotubes in solutions by an applied external magnetic field. To demonstrate the field-assisted alignment, we placed 10 mm quartz cuvettes filled with aqueous functionalized nanotube solutions (0.10 and 0.025 mg mL^{-1} CNT-$(COOH)_n$ in water) in the bore of an electromagnet and measured the field dependence (B up to 1017 mT) of optical transmission through the solutions at various optical polarization angles in reference to the magnetic field direction ($0° \leq \varphi \leq 180°$), as shown in Figure 2.

Depending on the angle of laser beam polarization as well as the density of the applied magnetic flux, we could significantly modulate the transmitted laser beam intensity—in a reversible manner—without applying extremely high magnetic fields. For the solution of 0.025 mg mL^{-1}, the original zero-field transmission $T_0 = 38.6\%$ reduced to $T_\perp = 20.8\%$ for $\vec{E}\perp\vec{B}$ and increased to $T_\parallel = 54.8\%$ for $\vec{E}\parallel\vec{B}$ at 1017 mT. The optical dichroism[40] $\Delta A = A_\perp - A_\parallel = -\ln(I_\perp/I_0) - (-\ln(I_\parallel/I_0))$, where I_0, $I_\perp$, and $I_\parallel$ denote the

(36) Ellis, A. V.; Ingham, B. *J. Magn. Magn. Mater.* **2006**, *302*, 378.
(37) Beuneu, F.; Huillier, C. L.; Salvetat, J.-P.; Bonard, J.-M.; Forró, L. *Phys. Rev. B* **1999**, *59*, 5945.
(38) Shen, K.; Tierney, D. L.; Pietrass, T. *Phys. Rev. B* **2003**, *68*, 165418.
(39) Andersson, O. E.; Prasad, B. L. V.; Sato, H.; Enoki, T. *Phys. Rev. B* **1998**, *58*, 16387.
(40) Shobaki, J.; Manasreh, D.; Yusuf, N. A.; Abu-Aljarayesh, I. *IEEE Trans. Magn.* **1996**, *32*, 5245.

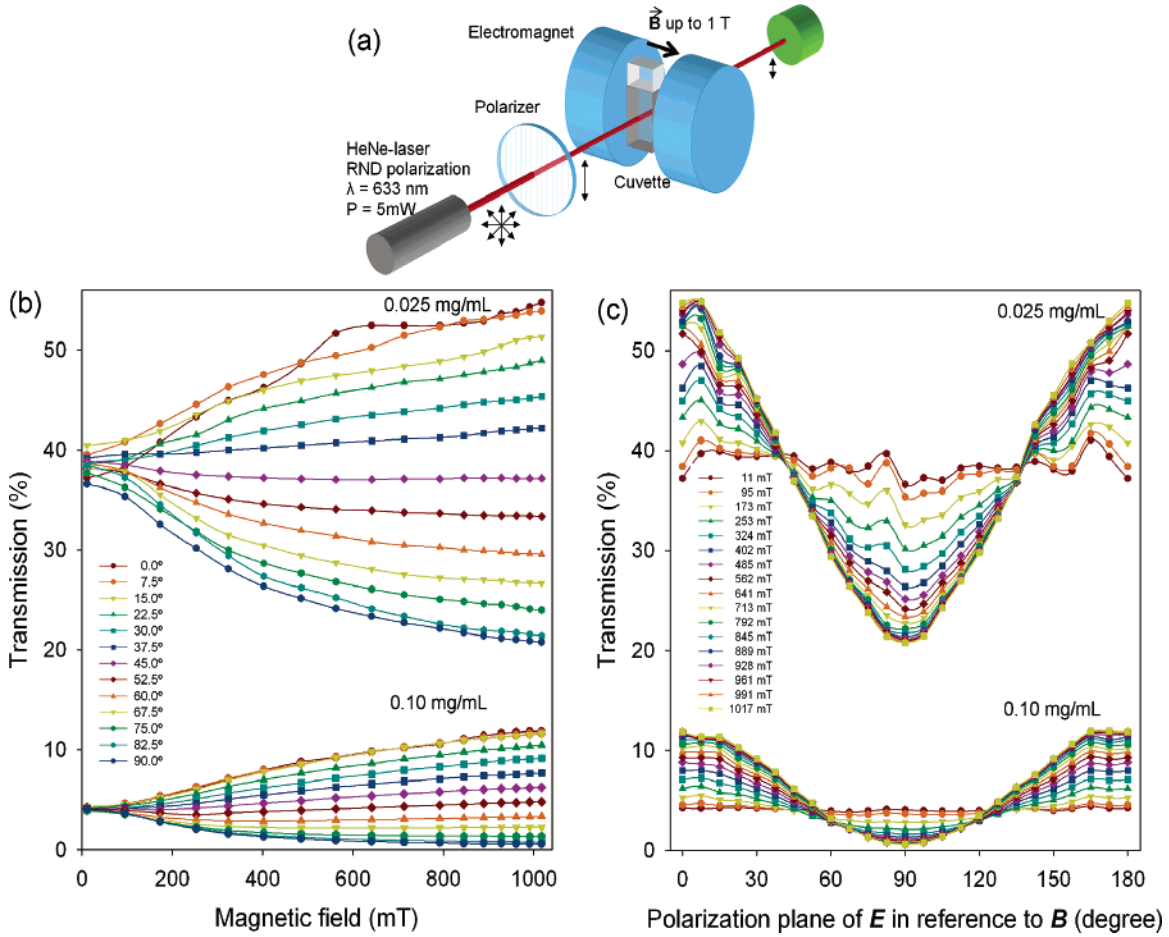

Figure 2. (a) Optical arrangement used for measuring optical transmission through nanotube solutions at room temperature in a magnetic field. The beam of a random polarized HeNe laser (JDS Uniphase 1125) is passed through a polarizer by which the polarization plane of $\vec{E}$ is set ($0° \le \varphi \le 180°$ in reference to $\vec{B}$). The transmitted power is measured by an optical multimeter (ANDO AQ2140) equipped with a detector (ANDO AQ2741). (b, c) Magnetic field and polarization vs optical transmission plots for aqueous CNT-$(COOH)_n$ solutions of 0.025 $g{\cdot}L^{-1}$ and 0.10 $g{\cdot}L^{-1}$ concentration.

transmitted intensities in zero field, field perpendicular, and parallel to the laser polarization, respectively, thus becomes ~0.97. The magnetic flux density vs transmission curves show a monotone increment with a slight saturation at ~1 T.

The situation was somewhat different for the less-diluted solution. Because of the large absorption and scattering (T_0 = 4.1%), the absolute values of the induced transmission change were much lower than those for the corresponding diluted solution, showing a modulation between 0.6 and 11.8% of the transmitted intensity. However, the relative change in transmitted intensity with the angle of polarization is considerably higher for this solution, yielding $\Delta A \sim 3.02$.

The obtained optical anisotropies suggest very good field-induced ordering, which is due to the large magnetic polarization of the entrapped iron nanoparticles in CNTs. To give a quantitative account for the ordering phenomenon, let us consider the magnetic potential energy $U = -M\rho VB\cos\theta$ of a nanotube of M mass magnetization, ρ density, V volume, and an angle θ between the nanotube axis and the magnetic field. The energy difference between randomly oriented and parallel aligned nanotubes thus becomes $\Delta U = -M\rho VB$. For a nanotube with 0.12 emu g^{-1} average magnetization, 3×10^{-6} m length, 4×10^{-8} m diameter, and 2.2×10^3 kg m^{-3} density, we get $\Delta U \approx -10^{-18}$ J at a magnetic flux density of 1 T. A nanotube has two rotational degrees of freedom; thus, when the principle of equipartition is applied, the kinetic rotational term becomes $E_{kin} = kT$. E_{kin} is $\sim 4 \times 10^{-21}$ J at 295 K, which is much lower than the value obtained for the potential term, i.e., the kinetic vibration is well-suppressed by the magnetic alignment. Now, by introducing $\alpha \equiv \Delta U/E_{kin}$, the nematic order parameter is calculated considering a single-parameter orientation model[26] $S = \int_{-1}^{1} f(\theta)((-1 + 3\cos^2\theta)/2)d(\cos\theta)$, where $f(\theta) = e^{-\alpha\ \cos^2\theta}/\int_{-1}^{1} e^{-\alpha\ \cos^2\theta}d(\cos\theta)$. We get $S \approx 0.99$, meaning an excellent alignment of the nanotubes in the applied (relatively moderate) magnetic field at room temperature.

It is important to point out that the nematic order parameter we obtained reflects an average figure, because the mass magnetization we measured for the acid-treated CNTs is a statistical average value. In reality, the ordering parameter for a nanotube depends on the amount of iron entrapped in the particular nanotube. For CNTs without encapsulated iron catalyst particles, the magnetization shows paramagnetic behavior[9,29] and is several orders of magnitude lower, typically on the scale of 1×10^{-5} emu g^{-1}, than the value we obtained by the SQUID analysis. Therefore, for pure nanotubes, the ordering parameter becomes $S \approx -0.48$, i.e. field-assisted alignment with the applied low magnetic fields cannot be achieved.

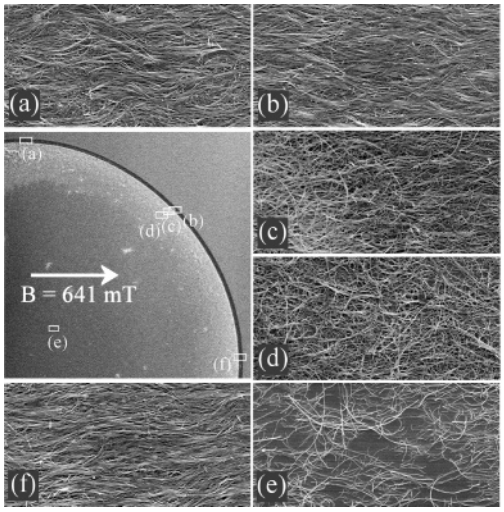

Figure 3. FESEM images of a dried CNT-$(COOH)_n$ solution droplet deposited on a polished Si surface. When drying, a magnetic field of 641 mT is applied that has a direction as indicated in the main panel (low magnification image, frame size 2.5 × 2.5 mm^2). (a−f) Higher-magnification images taken from selected areas (frame size 14 × 7 μm^2 each) of the dried solution droplet. (a, b, f) Well-aligned nanotubes around the perimeter. (c) Transition zone of random (on the left) and aligned CNT networks (on the right). (d, e) Tangled random networks with gradually decreasing surface coverage in the locations toward the center of the droplet.

The above-discussed heterogeneous nature of magnetization can be demonstrated by depositing and drying a droplet of CNT-$(COOH)_n$ solution on a polished Si wafer placed in a magnetic field. Field-emission scanning electron microscopy (FESEM, Jeol 6300-F) imaging of the dried deposits shows that a fraction of nanotubes aligns along the direction of the magnetic field, whereas the rest of the CNTs form a randomly oriented tangled network on the surface (Figure 3).

With the evaporation of the solvent, the nanotubes form a disc-shaped deposit pattern with a CNT ring of high surface coverage along its perimeter. In addition, this ring consists of two particular concentric zones: an outer one with well-aligned nanotubes being parallel with the applied magnetic field, and an inner ring with randomly oriented tangled networks of CNTs. (The orientation of nanotubes in the center of the disc is also random.) The formation of a characteristic annular deposit pattern is explained by a capillary flow, in which pinning of the contact line of the drying drop ensures that liquid evaporating from the edge is reloaded by liquid from the interior. The resulting outward flow carries the particles to the edge, resulting in the enrichment of dissolved particles along the droplet perimeter.[41] The reason for having two zones in this ring is the that magnetic field aligns the transported nanotubes with iron impurities and, in turn, those stick together by mutual magnetic attraction. The stacked nanotubes form large agglomerates and therefore cannot be circulated by the capillary flow near the drop edge, resulting in a sedimentation/deposition of such particles; however, the individual nonmagnetic nanotubes remain mobile and deposit later, causing a segregation of magnetic and nonmagnetic carbon nanotubes. This latter segregation model is supported by EDX analyses showing iron at the aligned areas, whereas no traces of the catalyst contamination were found in the randomly oriented inner ring.

Conclusion

In this work, we show a method to induce efficient alignment of aqueous carboxyl-functionalized multiwalled CNTs by relatively low magnetic fields ($B \leq 1017$ mT). The process exploits the ferromagnetic behavior of iron nanoparticles entrapped in the inner-tubular cavity of nanotubes. Considerable optical anisotropy of nanotube solutions and deposition of aligned CNT networks from the solutions were demonstrated. The results suggest applications in magnetic actuators, switches, and optical coatings. Furthermore, the segregation of iron-contaminated magnetic and pure paramagnetic nanotubes poses an alternative to separate/clean nanotubes in magnetic field.

Acknowledgment. The authors thank the Academy of Finland (Project #209414), Finnish Funding Agency for Technology and Innovation (Tekes, Project #1015/31/05), the Research Foundation of Seppo Säynäjäkangas, the Swedish Governmental Agency for Innovation Systems (VINNOVA), and the Interconnect Focus Center New York for supporting this work.

Supporting Information Available: Figure S1. This material is available free of charge via the Internet at http://pubs.acs.org.

CM062196T

(41) Deegan, R. D.; Bakajin, O.; Dupont, T. F.; Huber, G.; Nagel, S. R.; Witten, T. A. *Nature* **1997**, *389*, 827.